INTURN 24-2 Elucidating the Nature of Neutrinos Using Collider Probes

Student: Junwen Diao[1]
Mentors: Sebastián Urrutia Quiroga[1]
[1]Institute for Nuclear Theory, University of Washington, Seattle, WA 98195, USA

September 18, 2024

Abstract

This report focuses on discovering the different nature of Dirac and Majorana-type neutrinos by reproducing the analysis presented in Ref. [3] on the nature of neutrinos—specifically whether they are Dirac or Majorana particles—using collider probes and computational simulations. Neutrinos are unique in the Standard Model due to their charge neutrality and the potential to be their own antiparticle if they are Majorana fermions. The discovery of neutrino oscillation and subsequent confirmation of neutrino mass has reignited debates regarding their fundamental nature. Utilizing the computational tool MadGraph, we replicate the original study's simulation of collision events to examine the kinematic distributions of sterile neutrinos in both Dirac and Majorana scenarios. Our reproduced results confirm the distinct signatures in angular and rapidity distributions, as described in the original work, which can be used to differentiate between Dirac and Majorana neutrinos in future collider experiments that is part of the discussion for potential new physics beyond the standard model.

1 Neutrino: Dirac or Majorana?

Neutrinos are among the most abundant elementary particles in the universe. They are charge-neutral, spin-1/2 particles that interact solely via weak and gravitational interactions. Because charged weak interactions couple only to left-handed chiral particles or right-handed antiparticles, all neutrinos are left-chiral, and all antineutrinos are right-chiral [4].
Before we dive right into the question, it is important to mention helicity, the projection of spin onto the neutrinos' momentum direction. For example, by having a left-handed helicity (spin-momentum anti-parallel) state particle, by CPT theorem, we know that there will be a corresponding right-handed helicity (spin-momentum parallel) state anti-particle-the particle's CP partner-with opposite charge and lepton number [6], the number assigned to leptons-the particles that do not interact via strong interactions-by giving leptons 1 and anti-lepton -1. Once it is discovered that the particle has mass, there will be a reference frame that the particle is in a right-handed helicity state, and the anti-particle is in a left-handed helicity state. For most of the fermions like electrons, this works perfectly well, but when it comes to neutrinos, there can be a different story. As a fermion, the neutrino's lack of electric charge makes it a unique case in the Standard Model: it could be a Majorana fermion, meaning it would be its own antiparticle, like photon, which means the CP conjugate of the neutrino can be the same object as the Lorentz pair of the neutrino, but no massive Majorana particle has ever been discovered. In contrast, all other fermions in the Standard Model are Dirac fermions, for which each particle has a distinct antiparticle with opposite physical charges.

In the context of the Standard Model, the neutrino is massless. This interpretation rendered the debate over whether they were Dirac or Majorana fermions more philosophical than physical, as a massless particle has only two degrees of freedom—the CP-conjugate pair—and there is no Lorentz-boosted frame in which a left-helicity state would become right-helical. The probability of observing a right-handed helicity neutrino is [4]:

$$P \propto \left(\frac{m_\nu}{E_\nu}\right)^2$$

where m_ν is the neutrino mass and E_ν is the energy of the neutrino. For a massive neutrino, there is a small but nonzero probability that the neutrino's helicity can flip due to the fact that it moves slower than the speed of light. A helicity flip is more likely when the particle is moving slowly.

However, the idea of massless neutrinos was overturned by the discovery of neutrino oscillations in experiments like Super-Kamiokande (1998) [5] and SNO (2001) [1]. The change in neutrino flavor as it travels through space indicates that different neutrino flavors have different mass states. To have such mass states differences, neutrinos must possess mass.

The realization that neutrinos have mass reopened the debate on whether they are Dirac or Majorana fermions. As Fig. 1 shows: if neutrinos are Dirac fermions, they have four degrees of freedom: the CP-conjugate pair and a Lorentz partner for each helicity state. If they are Majorana fermions, there are only two degrees of freedom: the neutrino is its own CP conjugate, and a Lorentz boost changes only its helicity.

$$\begin{array}{c} \nu_L \leftarrow \text{CP} \rightarrow \bar{\nu}_R \\ \updownarrow \text{“Lorentz”} \\ \nu_R \leftarrow \text{CP} \rightarrow \bar{\nu}_L \end{array}$$

(a) Dirac case

$$\begin{array}{c} \nu_L \leftarrow \text{CP} \rightarrow \nu_R \\ \updownarrow \text{“Lorentz”} \\ \nu_R \leftarrow \text{CP} \rightarrow \nu_L \end{array}$$

(b) Majorana case

Figure 1: Two different degrees of freedom. Extracted from Ref. [6].

An experiment that can reveal the Dirac or Majorana nature of neutrinos is the neutrinoless double beta decay experiment. In this process, two neutrons within a nucleus simultaneously decay into two protons, each emitting an electron and an electron antineutrino. If neutrinos are Dirac fermions, lepton number conservation will hold. However, if neutrinos are Majorana fermions—meaning the antineutrino is actually the neutrino itself—the neutrino pair effectively "annihilates" (exists only as a virtual particle pair that never physically manifests), resulting in lepton number violation of 2 units [6]. The technical difficulty of performing the experiment comes from the extremely small mass of the neutrino, as Fig. 2 shows. Any observable A (like helicity we used here) that can distinguish the Majorana/Dirac nature is proportional to the mass m_ν of the neutrino [6]:

$$A \propto \frac{m_\nu}{E}$$

So the problem can be easier to answer if the neutrino mass is greater.

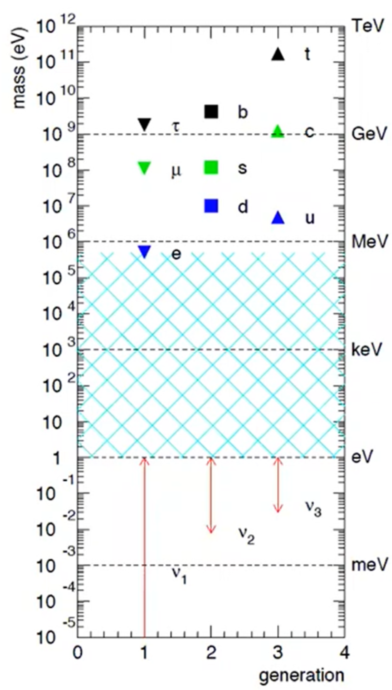

Figure 2: The energy scale of particles. Extracted from Ref. [6]

The Seesaw mechanism [7], a possible explanation for the origin of neutrino mass, predicts the existence of a heavy sterile neutrino (N) which is a great candidate and provides another potential solution to the problem. Consider the Dirac case in the processes $\ell^+\ell^- \to N\bar{\nu}_\ell$ and $\ell^+\ell^- \to \bar{N}\nu_\ell$, where ℓ^+ and ℓ^- are lepton and antilepton pairs, respectively. If the sterile neutrino (SN) is a Majorana fermion, then the $\bar{N}$ in the second process would also be N, as shown in the M2 scenario in Fig. 3. In the Dirac scenario, N tends to move in the direction of the ℓ^- (referred to as the forward direction) and decays into ℓ^- and W^+. Conversely, $\bar{N}$ tends to move in the direction of ℓ^+ (referred to as the backward direction), and decays into ℓ^+ and W^- [3] due to the parity nature of neutrinos. However, if N is a Majorana fermion, since $N \equiv \bar{N}$, the decay products ℓ^- and W^+ will appear in both the forward and backward directions [3]. Therefore, by identifying the region of discovery of ℓ^- and W^+ is crucial for distinguishing the Dirac or Majorana nature of neutrinos.

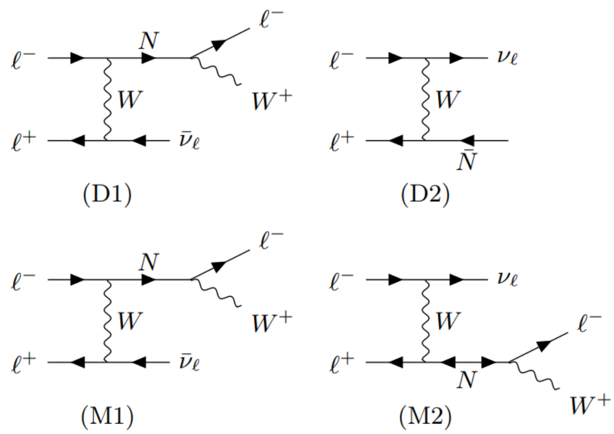

Figure 3: Feynman diagrams of the SN production and decay for (D) Dirac type N and (M) Majorana type N. Only the decay process with negative charged lepton ($\ell^- W^+$) is plotted. Extracted from Ref. [3].

2 MadGraph simulation

Our work on this stage will be based on Ref. [3]. We were trying to reproduce the analysis in the paper by using MadGraph [8], a powerful computational tool widely used in high-energy physics to efficiently generate and simulate collision events, providing valuable data for studying particle interactions and testing theoretical models. The lepton-anti-lepton pair used to generate the events were e^+ and e^-. MadGraph provides kinematic data for the particles in each event as shown in Fig. 4, allowing us to extract relevant information for further analysis.

```
<event>
 4      1 +4.5007000e+02 1.66666700e+03 7.81860800e-03 8.24324300e-02
      -11 -1    0    0    0    0 +0.0000000000e+00 +0.0000000000e+00 +1.5000000000e+03 1.5000000000e+03 0.0000000000e+00 0.0000e+00 1.0000e+00
       11 -1    0    0    0    0 -0.0000000000e+00 -0.0000000000e+00 -1.5000000000e+03 1.5000000000e+03 0.0000000000e+00 0.0000e+00 -1.0000e+00
       12  1    1    2    0    0 -1.1702613642e+01 +8.5880755407e+01 -1.3305131801e+03 1.3333333333e+03 0.0000000000e+00 0.0000e+00 -1.0000e+00
  9000005  1    1    2    0    0 +1.1702613642e+01 -8.5880755407e+01 +1.3305131801e+03 1.6666666667e+03 1.0000000000e+03 0.0000e+00 1.0000e+00
</event>
```

Figure 4: Kinematic information generated by MadGraph. The very first row shows the number of particles (4 in this example), the process ID, total energy (in GeV), largest z-component of momentum (in GeV), QED coupling α_{QED}, and QCD coupling α_{QCD}; from the second to the fifth row, the columns from left to right each represents: PDG code of each particle, particle status (-1 incoming, 1 outgoing, 2 intermediate), IDs of the parent particles from which this particle was produced, the two color charges information used in QCD processes, the four-momentum (P_1, P_2, P_3, P_0), mass (all in GeV), distance traveled (mm), and helicity. [2, 9]

We began by analyzing the events generated with the Dirac model by importing a pre-written file with all the parameters that tell MadGraph how a Dirac-type neutrino interacts. For simplicity, at this stage, the decay products of the heavy sterile neutrinos (SNs) were not considered. It is reasonable to predict that N and $\bar{N}$ are produced with equal probability and are distributed symmetrically in the forward and backward directions. To examine this, we can plot the distribution of $\cos\theta_N$, the angle between the SN and the ℓ^-.

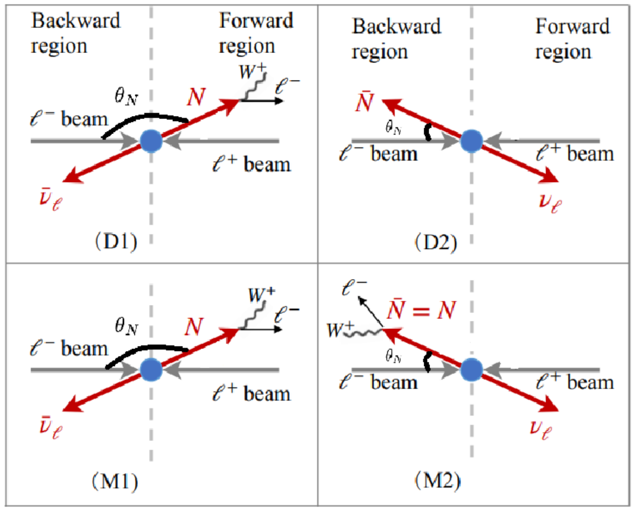

Figure 5: Illustration figure of the SN production. Dirac-type: only N can decay to $\ell^- W^+$ so ℓ^- are distributed in the forward region. Majorana-type: N and $\bar{N}$ are the same particles; therefore, they can decay to $\ell^- W^+$[3]. We believe that the θ_N in the original paper was incorrectly marked, so we remarked the θ_N based on the context. Extracted and modified from Ref. [3]

The symmetrical distribution of $\cos\theta_N$, as shown in Fig. 6, confirms that the Ns tend to move towards the forward region, while the $\bar{N}$s are directed towards the backward region, as expected. Since the SNs are much heavier than the νs, their scattering angles are likely to be close to 0.

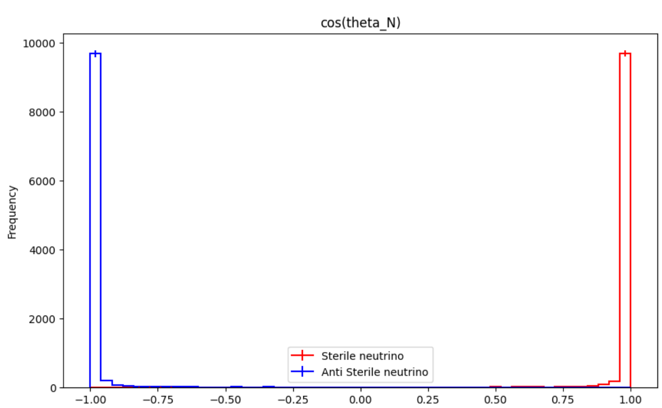

Figure 6: $\cos\theta_N$ distribution of Dirac-type SNs

We can then normalize the distribution by calculating the distribution of $\frac{1}{\sigma}\frac{d\sigma}{d\cos\theta_N}$. The differential cross section $\frac{d\sigma}{d\cos\theta_N}$ describe the rate at which scattering events occur with respect to the rapidity, which σ relates to the probability of an interaction happens and can be found by

$$\sigma = \int \frac{d\sigma}{d\cos\theta_N}\, d\cos\theta_N \tag{1}$$

which means that $\frac{1}{\sigma}\frac{d\sigma}{d\cos\theta_N}$ normalizes the distribution by describing the probability of finding a neutrino for a specific $\cos\theta_N$ and being integrated to be 1. The differential cross section of the SNs in the forward direction (D1 and M1 in Fig. 1) is [3]:

$$\frac{\mathrm{d}\sigma}{\mathrm{d}\cos\theta_N} = \frac{g^4|U_\ell|^2(1+\cos\theta_N)(s-m_N^2)^2}{64\pi s^2} \times \frac{(s+m_N^2+\cos\theta_N(s-m_N^2))}{[(s-m_N^2)(1-\cos\theta_N)+2m_W^2]^2}, \tag{2}$$

where g is weak coupling strength calculated to be 0.664 by using parameters in the model, U_i is a weight that shows how g is adapted for the lepton, s is the collision energy squared, m_N is the mass of SN, and m_W is the mass of the W boson. In our simulation, $\sqrt{s} = 3000$ GeV, $m_N = 1000$ GeV. We will replace $\cos\theta_N$ by $-\cos\theta_N$ for SNs going in backward direction (D2 and M2 in Fig. 1). The forward and backward direction differential cross sections equation is shown in Fig. 7. The linear combination of the two equations will provide us with the symmetrical plot we expected.

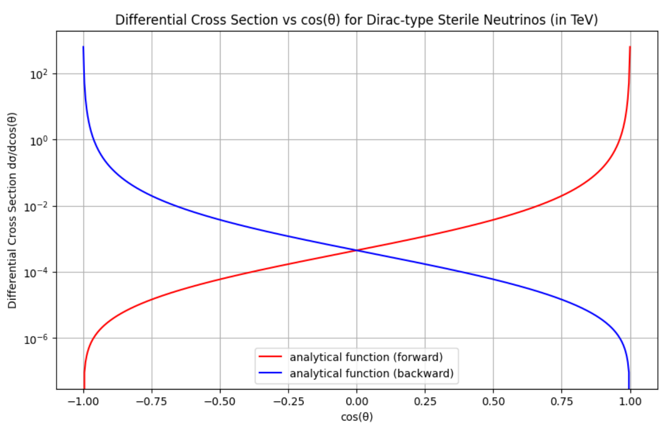

Figure 7: Analytic equations for forward and backward differential cross sections of Dirac-type SNs that provide the two peaks (log scale). For simplicity, U_ℓ is 1 in this plot.

To find the differential cross section for a group of events, since $\frac{1}{\sigma}\frac{d\sigma}{d\cos\theta_N}$ normalizes the distribution, we propose the differential cross section and the $\cos\theta_N$ distribution follow the relation $\frac{d\sigma}{d\cos\theta_i} = \lambda N_i$, where N_i and $\frac{d\sigma}{d\cos\theta_i}$ are the number of events and the distribution in the i-th bin, respectively. The following process can calculate the scaling factor λ:

$$\sigma = \sum_i \frac{d\sigma}{d\cos\theta_i}\Delta\cos\theta_i\ , \quad N = \sum_i N_i$$

$$\sigma = \Delta\cos\theta \sum_i \lambda N_i = \lambda\Delta\cos\theta N$$

$$\lambda = \frac{\sigma}{N\Delta\cos\theta_i}$$

where N is the total number of events. We have assumed that $\Delta\cos\theta_i \equiv \Delta\cos\theta$ is constant, so the width of each bin in the histogram is the same. This process shows the differential cross sections can simply be calculated from the counts from each bin of histogram and the cross section, which are accessible from the data generated by MadGraph. The scaled distribution of Dirac-type SNs are shown in Fig. 8a. By repeating the steps above for events generated with Majorana model, we see a symmetrical distribution where the Ns go to both forward and backward regions as shown in Fig. 8b due to the Majorana nature of $N \equiv \bar{N}$. This is a clear signal to distinguish the Dirac/Majorana nature of neutrino.

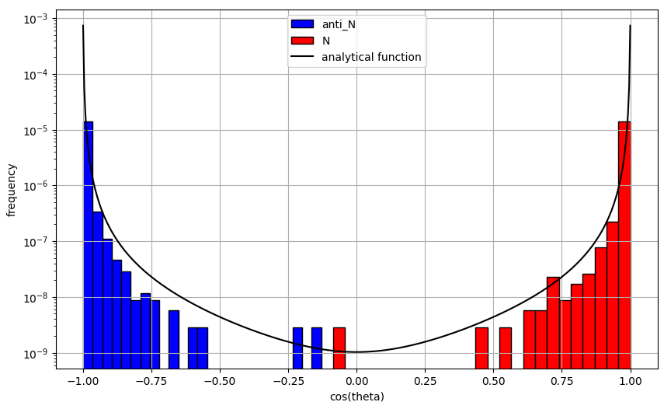

(a) Scaled $cos\theta_N$ distribution (Dirac)

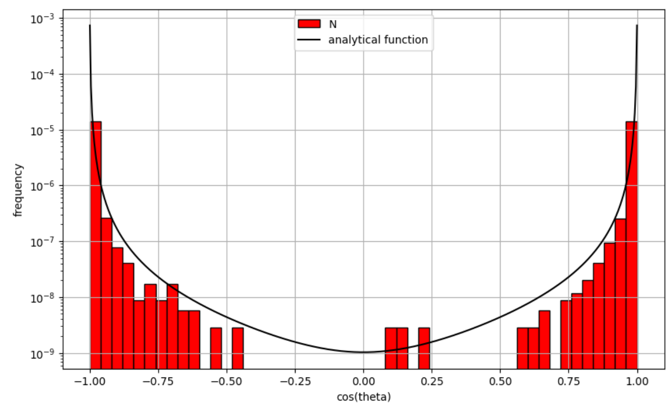

(b) Scaled $cos\theta_N$ distribution (Majorana)

Figure 8: Scaled $cos\theta_N$ distribution fitted with the analytic equation of differential cross section

We can also study the distribution of the rapidity y_N, a spacetime invariant version of $\cos\theta_N$ considering the relativistic effect due to the high speed motion of the particles. The rapidity y_N is defined as:

$$y_N = \frac{1}{2}\log\frac{E + p\cos\theta_N}{E - p\cos\theta_N} \tag{3}$$

where E and p are the energy and momentum of the SN, respectively. Consequently, y_N should have a similar distribution compared to $\cos\theta_N$ in the center-of-mass frame, as shown in Fig. 9.

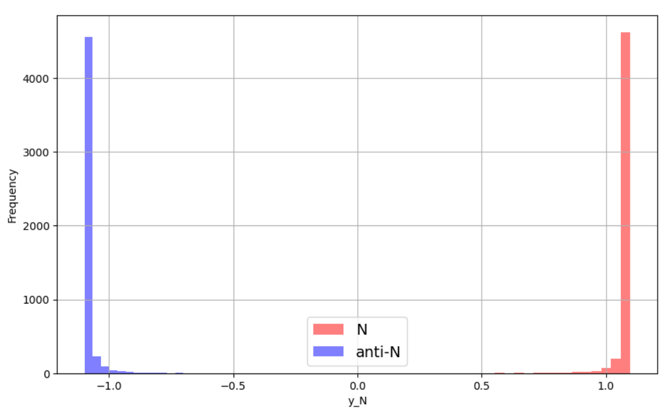

(a) y_N distribution (Dirac)

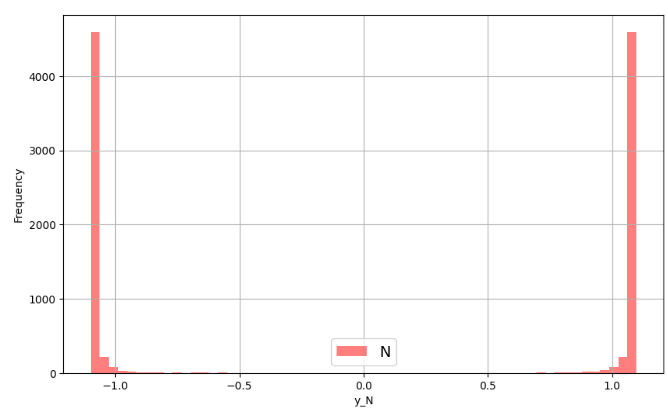

(b) y_N distribution (Majorana)

Figure 9: y_N distributions

We can use the same method to normalize the y_N distribution as we normalize the $\cos\theta_N$ distribution by replacing $\cos\theta_N$ in Eq. 2 by a function of y_N transformed from Eq. 3. But We encountered difficulties here since we were not able to transform Eq. 2 to the given form in Ref. [3] which shows that

$$\frac{\mathrm{d}\sigma}{\mathrm{d}y_N} \propto \frac{e^{4y_N}\left(se^{2y_N} - m_N^2\right)}{\left(e^{2y_N}+1\right)^2\left(s+m_W^2-e^{2y_N}\left(m_N^2-m_W^2\right)\right)^2} \tag{4}$$

But instead what we got was an ugly expression that we could not separate the variables that clean since we do not know what potential transformation is used by the paper that can help separating or eliminating the variables.

$$-\frac{g^4\left(\left(-1+e^{2y_N}\right)E+\left(1+e^{2y_N}\right)p\right)\left(m_N^2-s\right)^2\left(\left(-1+e^{2y_N}\right)E\left(m_N^2-s\right)-\left(1+e^{2y_N}\right)p\left(m_N^2+s\right)\right)|U_\ell|^2}{64\pi\left(\left(-1+e^{2y_N}\right)E\left(m_N^2-s\right)-\left(1+e^{2y_N}\right)p\left(m_N^2-2m_W^2-s\right)\right)^2 s^2} \tag{5}$$

This can be due to a lack of knowledge of what transformation is used. But we can still calculate $\frac{d\sigma}{dy_N}$ by directly using Eq. 4 to check the distribution. We were expecting to get a plot similar to Fig. 10.

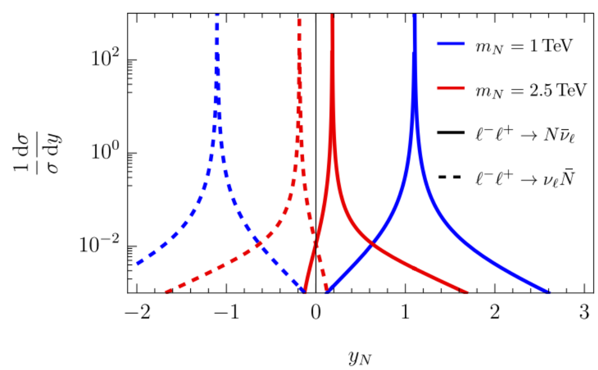

Figure 10: Normalized rapidity distribution of SNs in the paper, where the dashed line appears for Majorana fermions only. Extracted from Ref. [3].

And the plots we got from the data are shown in 11

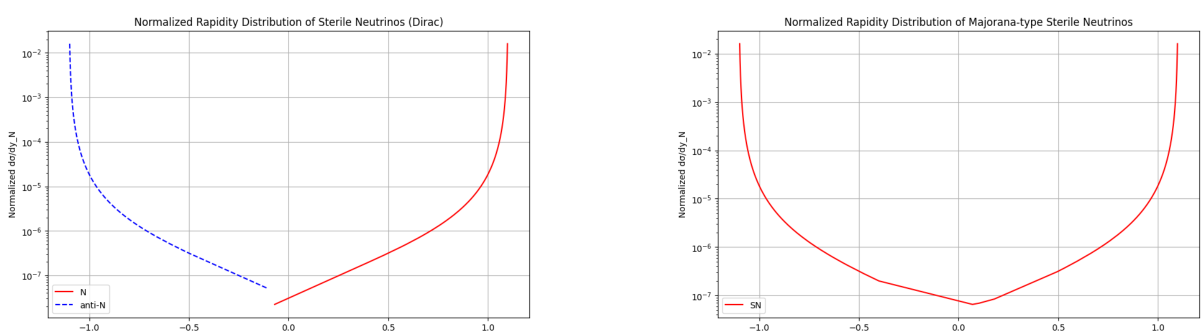

(a) Normalized y_N distribution (Majorana)

(b) Normalized y_N distribution (Majorana)

Figure 11: Normalized y_N distribution. For simplicity, U_l is set to be 1.

which has fits half of the graph given in the paper with the correct location of peak but without the tail on the other half. By constraining E and p in Eq. 3 by the invariant mass $E^2 - p^2 = m^2$, it seems to be impossible for y_N to go even beyond 2 with collision energy being 3 TeV.

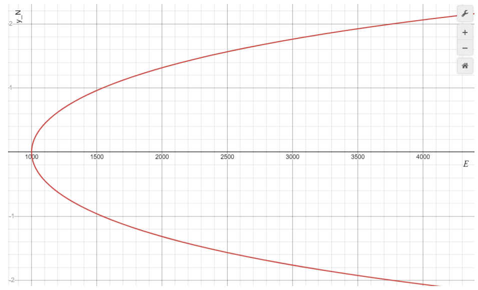

Figure 12: y_N as a function of E, p, and $\cos\theta_N$, where p is constrained by $E^2-p^2 = m_N^2$. The x-axis represents E and y-axis represnts y_N. The two curves shows the two extremes, where $\cos\theta_N = \pm 1$. It shows that even the SN takes all of the collision energy 3 TeV, y_N will not even go beyond 2.

But again, this can be due to a lack of information on what the authors of Ref. [3] used. So instead of using $\frac{d\sigma}{dy_N}$ which we have a lack of understanding, we chose to focus on the distribution of $\cos\theta_N$, which has a clear domain of $(-1, 1)$.

3 What's next

In practice, neutrinos are not detected directly, so the kinematic information comes from conservation laws and the decay products. The next step the decay process of the SNs will be added and the rapidity will be calculated by the kinematics information of the decay product (the $\ell^- W^+$). For the purpose of theoretical analysis, we removed all the cuts in the simulation, which will be a practical consideration. The sensitivity is a potential factor in our analysis.

Acknowledgement

This research was supported by the INT's U.S. Department of Energy grant No. DE-FG02-00ER41132 and the N3AS's National Science Foundation award No. 2020275.

References

[1] Q. R. Ahmad et al. "Measurement of the Rate of $\nu_e + d \to p + p + e^-$ Interactions Produced by ^8B Solar Neutrinos at the Sudbury Neutrino Observatory". In: Physical Review Letters 87.7 (2001), p. 071301. DOI: 10.1103/PhysRevLett.87.071301.

[2] E. Boos et al. "Generic User Process Interface for Event Generators". In: (2001). arXiv: hep-ph/0109068 [hep-ph]. URL: https://arxiv.org/abs/hep-ph/0109068.

[3] Qing-Hong Cao, Kun Cheng, and Yandong Liu. "Distinguishing Dirac/Majorana Heavy Neutrino at Future Lepton Colliders". In: (Mar. 2024). arXiv: 2403.06561 [hep-ph].

[4] E. Conley et al. Chirality and Neutrinos. Presented at the Fermilab Neutrino Physics Conference. Accessed: 2024-09-11. n.d. URL: https://indico.fnal.gov/event/13429/contributions/19334/attachments/12692/16078/neutrinos_slides.pdf.

[5] Y. Fukuda et al. "Evidence for Oscillation of Atmospheric Neutrinos". In: Physical Review Letters 81.8 (1998), pp. 1562–1567. DOI: 10.1103/PhysRevLett.81.1562.

[6] Andre Luiz de Gouvea. Majorana or Dirac, That is the Question 6-3-21. Online; accessed 5-September-2024. YouTube, https://www.youtube.com/watch?v=vo05ctycro0. 2021.

[7] P. Minkowski. "$\mu \to e\gamma$ at a Rate of One Out of 10^9 Muon Decays?" In: Physics Letters B 67.4 (1977), pp. 421–428. DOI: 10.1016/0370-2693(77)90435-X.

[8] Jorge C. Romão. "Short Usage Introduction to MadGraph 5". In: (2022). Presented on January 24, 2022. URL: https://porthos.tecnico.ulisboa.pt/CTQFT/files/MadGraph5.pdf.

[9] Yi-Ming Zhong. Hands-on Start to MadGraph. 1st Workshop on New Light Physics and Photon-beam Experiments. Available at: https://github.com/ymzhong/mg5_aMC_tutorial. 2021. URL: https://indico.jlab.org/event/413/contributions/7694/attachments/6580/8909/Hands-onStartToMG.pdf.